1 PAW functions for the actinoids

1.1 Introduction

Today, there are a number of reliable and efficient pseudopotential databases that cover a large part of the periodic table and are compatible with the common open-source PP-PW software packages for solid-state calculations. Examples are the *SG15 Optimized Norm-Conserving Vanderbilt Pseudopotentials*[1], die *GBRV High-Throughput Database*[2] for USPP's or the *Pslibrary*[3] for PAW data sets. Standardized test calculations and convergence studies are available for these and other data sets on the *Materialscloud* server under the *Standard Solid-State Pseudopotentials*[4] (SSSP) project. However, basic sets for the actinoids are missing in this compilation. Only the *Pslibrary* lists USPP and PAW data sets for Th to Pu. These basis sets are very hard requiring cutoff energies of up to more than 100 Ry, are difficult to converge and also show numerical instabilities in initial tests. Therefore, we created a new set of scalar- and fully-relativistic PAW functionals for the actinoids Th to Lr in the GGA-PBE and the LDA-PW approximation in this PhD thesis. The results are analogous for both functionals and are presented only for the PBE calculations.

1.2 Generation of the PAW functions

1.2.1 General procedure

The PAW data sets were generated using the *Atomic* program of the *Quantum ESPRESSO* software package.[5,6] The technical procedure and strategy of parameter selection is taken from the methodology for the generation of the *Pslibrary* and was slightly modified for the requirements of this work.[3] The procedure is automated in the *Atomic* code except for the parameter selection and will now be presented.

First, self-consistent atomic all-electron (AE) calculations were performed for the given reference electron configuration to obtain the AE potential, the radial AE wave functions and the eigenvalues of the bound reference states. The electron configurations of the free actinoid atoms were chosen as reference electron configurations for the PAW basis functions. The fully-relativistic PAW functions including SOC were generated with slightly ionic configurations whose charge increases with increasing atomic number Z from $+0.1$ to $+0.6$. For this, the 7s orbitals or the 5f orbitals were partially occupied. For Lr atoms, the inclusion of SOC leads to a rearrangement of the atomic electronic configuration[7] from $[\mathrm{Rn}]7\mathrm{s}^2\,7\mathrm{p}^0\,6\mathrm{d}^1\,5\mathrm{f}^{14}$ in the sr approximation to $[\mathrm{Rn}]7\mathrm{s}^2\,7\mathrm{p}^1\,6\mathrm{d}^0\,5\mathrm{f}^{14}$ in the fully-relativistic basis with SOC. For all PAW basis functions generated, the 6s and 6p semicore orbitals were considered as valence orbitals.

The local part of the PAW potentials was generated from the AE potentials according to the method of Troullier and Martins.[8] The selected core radius of the potentials $r_{\mathrm{c,loc}}$ decreases with increasing Z from 1.5 a.u. to 1.2 a.u.

The bound AE states were extended by unbound states at reference energies E_l in order to increase the transferability of the basis functions. Taken together, they form the set of partial waves ϕ_i^{AE}. For each angular

momentum component up to $l_{\max} = 3$ two partial waves were used. Partial pseudo-waves ϕ_i^{PS} with core radius r_{c} were generated according to the polynomial method of Troullier and Martins.[8] The values of r_{c} are identical for partial pseudo-waves with the same l with two exceptions. For the unbound 5f partial waves, r_{c} is larger than for the bound 5f partial waves to improve the convergence properties. In the case of the fully-relativistic basis functions, the values of r_{c} of the $7\mathrm{p}_{3/2}$ waves are 0.1 a.u. larger than r_{c} of the $7\mathrm{p}_{1/2}$ waves to maintain the stability of the PAW basis.

The projectors[9] $\beta_i(r)$ and the augmentation functions[10] $Q_i(r)$ for the compensating charges of the valence charge density were generated from the pseudowaves. The augmentation functions were generated from the origin to $r_{\mathrm{c,aug}}$ from the AE augmentation via three Bessel functions. For each partial pseudo-wave, an individual value of $r_{\mathrm{c,aug}}$ was chosen, where $r_{\mathrm{c,aug}} < r_{\mathrm{c}}$.

The non-linear core correction was used for all PAW basis functions.[11] For this purpose, the real core charge from the origin up to $r_{\mathrm{c,c}}$ was replaced by a pseudo-core charge built from Bessel functions. The value of $r_{\mathrm{c,c}}$ was chosen so that the radial dependence of the real core charge is well reproduced by the pseudo core charge from $r \approx 0.5$ a.u. onwards.

1.2.2 Parameter optimization

The hardness and transferability of the PAW basis functions of the actinoides are mainly controlled by the core radii r_{c} of the 5f partial pseudo-waves. It turns out that the transferability of the basis is mainly determined by r_{c} of the bound 5f pseudo-waves and the hardness is mainly influenced by r_{c} of the *unbound* 5f pseudo-waves. By using two different values of r_{c}, hardness and transferability can be optimized. A larger value for r_{c} of the unbound 5f pseudo-waves is favorable here. An additional

positive influence on the transferability is the selection of the smallest possible value for the core radius of the local potential $r_{\mathrm{c,loc}}$.

In addition to hardness and transferability, the numerical stability of the basis functions was also tested and optimized. The number of diagonalisation cycles required in *Quantum ESPRESSO* for the SCF convergence of an fcc structure of the elementary actionides was chosen as a test criterion. Improved numerical stability was primarily achieved by changing the shape of the projectors $\beta_i(r)$ and the augmentation functions $Q_i(r)$. Small absolute function values of $\beta_i(r)$ in the order of the magnitude of the partial waves $\phi_i^{\mathrm{PS}}(r)$ prove to be favorable. This can be achieved by increasing the reference energies E_l of the unbound states. Small absolute values of the augmentation functions $Q_i(r)$ are also favorable and, in addition, a reproduction of the largest maximum of the AE augmentation by the PS augmentation functions that is as good as possible. Both can be achieved by reducing E_l and the core radii $r_{\mathrm{c,aug}}$. In terms of the projectors, a compromise is therefore necessary for the choice of E_l. Reducing the core radii $r_{\mathrm{c,aug}}$ leads to an increase in the required cut-off energy of the charge density. The AE augmentation applied here allows the use of the basis sets as USPPs. For PAW data sets, the shape of the augmentation functions is less important than for USPPs. In the PAW formalism, the choice of $Q_i(r)$ should only ensure that no negative charges arise in real space in later calculations, which can lead to convergence difficulties.[3] The effect of using smoother augmentation functions on the efficiency of the PAW basis remains to be examined.

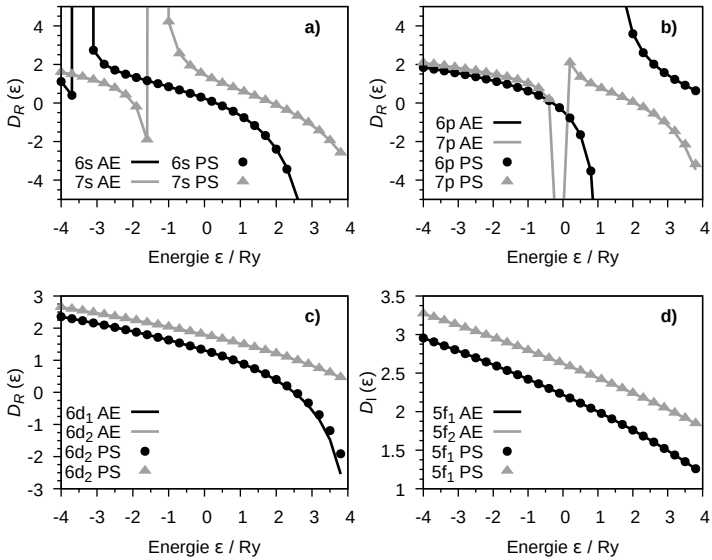

Abbildung 1.1: Scattering $D_R(\epsilon)$ at the diagnostic radius $R = 2.2$ a.u. of the different angular momentum components l of the scalar-relativistic PBE-PAW basis of the uranium atoms . **(a)** $l = 0$, **(b)** $l = 1$, **(c)** $l = 2$ and **(d)** $l = 3$. AE calculations (AE), PAW calculations (PS).

1.3 Testing the PAW functions

1.3.1 Atomic calculations

The quality and transferability of the created PAW basis functions were examined in a first step in atomic test calculations with the *Atomic* code. For this purpose, the scattering behaviour $D_R(\epsilon)$ was checked optically at a diagnostic radius $R = 2.2$ a.u. in order to estimate the transferability of the basis. For the scalar-relativistic basis of the uranium atoms, $D_R(\epsilon)$ is shown for the different angular momentum components l in Figure 1.1. For the investigated energy range of -4 Ry $< \epsilon < 4$ Ry, the basis shows good transferability. The AE data (lines) are reproduced by the PAW

data (points) over almost all values of ϵ. For the components $l = 1$ and $l = 2$, a deviation is observed from about 3.5 Ry. Similar observations can be found in the other PAW basis sets of this work.

In further tests, the total energy E and the eigenvalues ϵ were calculated for different reference electron configurations and were compared with AE data. A total of three ionic configurations with a charge of +1, +2 and +3, as well as two neutral configurations were examined. The strongest, although not critical, deviations from the AE results are found in the test calculations with the highest charge of +3. Here, the reference electron configurations [Rn]$7s^0$ $7p^0$ $6d^{m-1}$ $5f^n$, and [Rn]$7s^0$ $7p^0$ $6d^m$ $5f^{n-1}$ were chosen. For actinoide atoms that have m electrons in the d orbitals and n electrons in the f orbitals in the atomic ground state, the former configuration was chosen, for all other actinoide atoms the latter. The non-compensated nuclear charge in the ionic configurations leads to a contraction of the valence orbitals in comparison with the neutral generation configuration of the basis functions. This influences the transferability, especially the eigenvalues ϵ_{5f} of the localized 5f orbitals. Their difference from the AE calculations $\Delta\epsilon_{5f}$ is listed in Figure 1.2(a). Triangles represent test results of the scalar-relativistic basis, circles those of the fully-relativistic basis. Both sets of basis functions give a similar error range. For some of the basis functions (Pa, U, Np, Cm, Cf, Lr), the eigenvalue error $\Delta\epsilon_{5f} \leq 1$ mRy is very small despite the high charge of the reference electron configuration. For the other basis functions, $\Delta\epsilon_{5f}$ is between 3 mRy (Th) and 6 mRy (Fm). It is striking that the fully-relativistic basis functions partially reduce the error of the scalar-relativistic basis functions. This is probably due to the twice as much projectors of the fully-relativistic basis, since here each angular momentum component $l > 0$ has four projectors, two for each total angular momentum j. The difference of the total energy $\Delta E$of the PAW and AE calculations is listed in Figure 1.2(b). For a large part of the basis sets

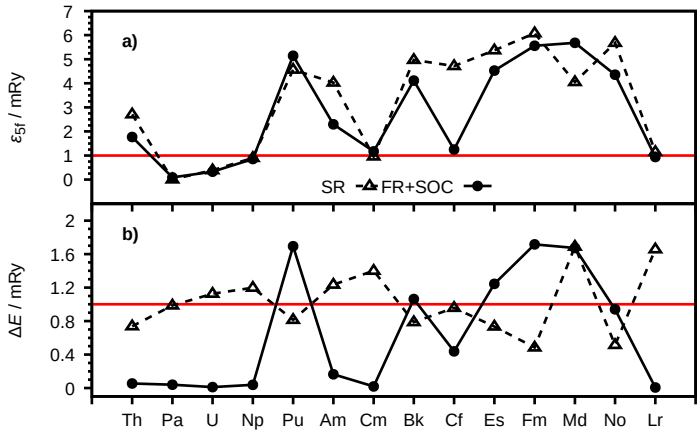

Abbildung 1.2: Atomic tests of the scalar-relativistic (SR, triangles) and fully-relativistic (FR+SOC, dots) PBE-PAW basis functions of the actinoids against AE data. Results of triply positively charged ions (see text). **(a)** Difference of the 5f eigenvalues $\Delta\epsilon_{5f}$ **(b)**Difference of the total energy ΔE.

this difference is close to $\Delta E = 1\,\text{mRy}$, which indicates excellent tranferability. For Pu, Fm, Md and Lr, the error approaches $\Delta E = 2\,\text{mRy}$. As in the case of the 5f eigenvalues ϵ_{5f}, also for the total energy the error of the fully-relativistic PAW basis is reduced compared to the scalar-relativistic basis. This is especially the case for the basis sets for the early actinoids up to Cm. Here, ΔE reduces to near zero. An exception is the fully-relativistic basis set for Pu, for which $\Delta E = 1.7\,\text{mRy}$ is calculated. The causes for this outlier still have to be investigated in detail.

1.3.2 Solid-state test calculations

In a second round of testing, the PAW functions were tested on simple solid structures. For this work, fcc and bcc packing variants were chosen. First, the basis set convergence was investigated. For this purpose,

the required value of E_{cut} for the representation of the wave function was determined in order to achieve convergence of the total energy ΔE to 1.5 mRy, of the cell pressure Δp to 1.5 GPa and the bcc-fcc transformation enthalpy ΔH to 0.05 kJ mol^{-1}. The number of plane waves for the charge density and potential was set to $8 \cdot E_{\mathrm{cut}}$. The results of the convergence tests are listed in Table 1.1 and are compared with the results from Dal Corso.[3] The least demanding E_{cut} is needed for the convergence of ΔH, followed by ΔE. The most difficult to converge is the pressure Δp, which is important for variable-cell optimizations. The scalar-relativistic and fully-relativistic basis sets generally yield similar convergence criteria. Roughly, the required value of E_{cut} increases with increasing atomic number Z, starting with values between 30 Ry and 50 Ry for Th and ending with values from 60 Ry to 80 Ry for Lr. The most difficult convergence behaviour is shown by No, for which a cutoff of 90 Ry is required for convergence of total energy and pressure. The increasing hardness of the basis functions with increasing Z results primarily from contraction the 5f orbitals. The position of the outer maximum of the radial functions decreases by about 0.4 a.u. from Th to Lr. To ensure transferability, the core radii r_{c} of the 5f orbitals must be reduced, which complicates the overall convergence. The choice of a relatively small value of $r_{\mathrm{c,5f}} = 1.3$ a.u. is the reason for the increased convergence requirements of the PAW functions of Th, Pa, U and Np by Dal Corso.[3] The required values of E_{cut} are up to 50 Ry larger than for the corresponding basis functions from this thesis.

The PAW data sets were further tested against LAPW+LO calculations using the *Elk* code. For better comparability, the tests were carried out without spin polarization. The equilibrium atomic volume V_{A}, as well as the bulk modulus K of bcc structures of the actinoide elements were determined. The results of the scalar-relativistic PAW and AE calculations are compared in Figure 1.3(a) and (b). The PAW and LAPW+LO

Tabelle 1.1: E_{cut} convergence in Ry of the actinoid PAW basis sets of this work (MS) for selected properties of PBE calculations of bcc- and fcc structures. Reference basis sets from Dal Corso (DC):[3] Convergence of the total energy ΔE to 1.5 mRy, the cell pressure Δp to 1.5 GPa and the bcc-fcc transformation enthalpy ΔH to 0.05 kJ mol^{-1}. Calculations without (SR) and with SOC.

Element	Basis	ΔE		Δp		ΔH	
		SR	SOC	SR	SOC	SR	SOC
Th	MS	40	50	40	50	30	50
	DC	80	–	80	–	90	–
Pa	MS	50	50	50	50	50	50
	DC	90	–	90	–	80	–
U	MS	60	60	70	70	60	70
	DC	110	–	100	–	90	–
Np	MS	70	70	70	70	70	70
	DC	120	–	120	–	120	–
Pu	MS	70	60	80	70	80	60
	DC	60	–	70	–	60	–
Am	MS	70	70	70	70	70	70
Cm	MS	70	70	70	70	70	70
Bk	MS	70	70	80	80	70	70
Cf	MS	70	80	80	80	50	80
Es	MS	70	80	80	80	60	50
Fm	MS	70	80	70	80	60	50
Md	MS	80	80	80	80	70	50
No	MS	90	90	90	80	70	50
Lr	MS	80	70	80	80	70	60

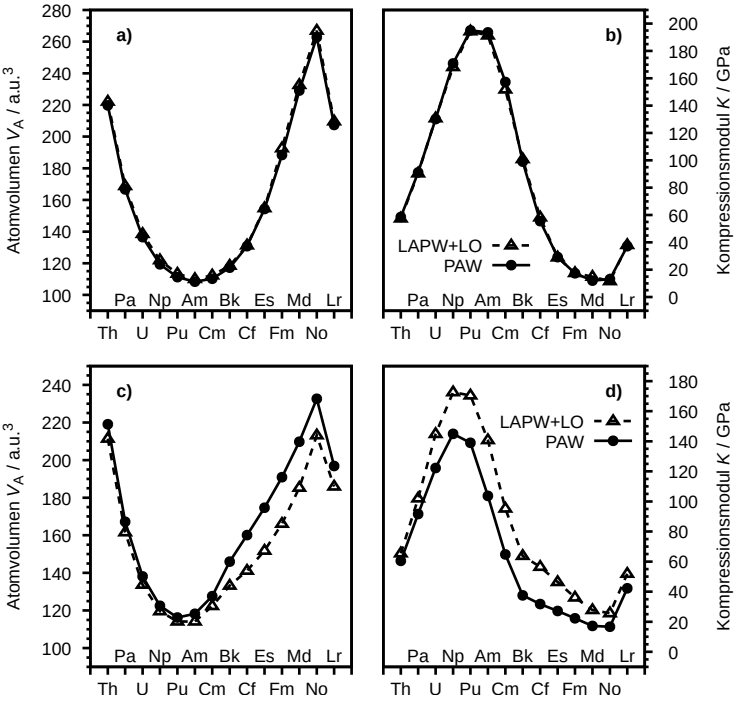

Abbildung 1.3: Comparison of PBE calculations on bcc structures of actinoids with PAW basis (dots) and LAPW+LO basis (triangles). **(a)** Equilibrium atomic volume V_A and **(b)** bulk modulus K (scalar-relativistic). **(c)** V_A and **(d)** K (Calculations with SOC).

data of the most elements show excellent agreement for V_A as well as for K. The deviations for V_A are a maximum of 4 a.u.^{3} in absolute terms and between 1 % and 2 % in relative terms. The differences for K amount to a maximum of 5 GPa in absolute terms and are about 5 % in relative terms. Two exceptions are Md with $\Delta K = 19\,\%$ and No with $\Delta K = 12\,\%$.

The data sets show clear differences when taking SOC into account. The results are summarized in Figure 1.3(c) and (d). The agreement of V_A is still relatively good for the light actinoides Th to Am with relative deviations between 2 % and 4 %. The differences increase for the other actinoids and are at a maximum for Es with $\Delta V_A = 15\,\%$. The absolute differences of K range between 5 GPa for Th and have an almost v-shaped maximum of 37 GPa for Pu. The relative deviation increases up to 43 % at Bk. The reason for these pronounced deviations is probably the different implementation of SOC interactions in the PAW and LAPW+LO formalisms. In the LAPW+LO code, SOC effects are introduced by perturbation theory via a second variational approach.[12] In DFT calculations on the light actinoids, this leads to inaccurate equilibrium volumes and convergence difficulties of the total energy.[13] This can be remedied by extending the scalar-relativistic basis by $6p_{1/2}$ basis functions.[14] However, this correction is not implemented in the *Elk* code. The fully-relativistic PAW basis integrates SOC effects via coefficients in the PAW potential. It thus should not have the limitations of the LAPW basis.[15]

1.3.3 Comparison with literature

Finally, the generated basis sets are to be compared with literature data. For this purpose, PBE calculations without spin polarisation on fcc element structures with the scalar- and fully-relativistic basis with SOC were selected. For the scalar-relativistic calculations, the values for V_A

Tabelle 1.2: Comparison of scalar-relativistic PBE calculations on fcc structures of actinoids with literature data from PAW[3] and LAPW+LO calculations[16]: Equilibrium atomic volume V_A, bulk modulus K.

Größe	Basis	Element				
		Th	Pa	U	Np	Pu
V_A/ a.u.^{3}	PAW†	216.3	170.7	146.3	129.5	119.3
	PAW[3]	216.5	170.3	146.1	129.7	119.7
	LAPW†	217.2	172.8	148.1	131.1	120.5
	LAPW[16]	219.2	172.3	147.5	131.4	122.3
K / GPa	PAW†	55.5	95.0	117.7	137.1	152.9
	PAW[3]	55.3	94.9	117.4	138.5	154.1
	LAPW†	56.0	94.7	117.8	140.7	170.4
	LAPW[16]	57.1	94.8	117.0	137.0	153.0

† Data from this PhD thesis.

and K are listed in Table 1.2. In addition, the results of the LAPW+LO calculations of this work and corresponding reference data are given. Both PAW data sets show a good agreement with a maximum relative deviation of $V_A = 0.3\,\%$ for Pu and $\Delta K = 1.0\,\%$ for Np. The LAPW+LO data sets also give similar values to each other and to the PAW data. The bulk moduli of Np and Pu calculated with the LAPW+LO basis from this work are striking as they deviate by up to 11 % from the literature data. The reason for this was not investigated further.

The results for V_A and K of the calculations with SOC are compiled with the literature values in Table 1.3. Both PAW data sets provide good agreement for V_A, again. However, the deviations in the calculated values for K increase in comparison to the scalar-relativistic calculations. The relative error ΔK for Pu is 4.9 %. The strong differences within the LAPW+LO calculations are striking. The value of V_A varies by up to 10.6 a.u.^{3} for Th, the value of K up to 22.5 GPa for U. These differences

Tabelle 1.3: Comparison of fully-relativistic PBE calculations on fcc structures of actinoids with literature data from PAW[3] and LAPW+LO calculations[16]: Equilibrium atomic volume V_A, bulk modulus K.

Größe	Basis	Element				
		Th	Pa	U	Np	Pu
V_A/ a.u.^{3}	PAW†	216.9	171.7	149.5	136.1	131.3
	PAW[3]	216.6	171.5	149.2	136.2	131.7
	LAPW†	207.5	165.8	144.1	130.9	125.2
	LAPW[16]	218.1	172.8	148.7	137.9	133.4
K / GPa	PAW†	59.2	96.0	108.7	108.4	86.6
	PAW[3]	58.0	95.8	109.2	109.4	91.1
	LAPW†	64.2	102.4	121.5	131.3	117.9
	LAPW[16]	73.1	96.0	99.0	140.0	121.0

† Daten aus dieser Doktorarbeit.

as well as the discrepancy with respect to the PAW results are probably due to the difficult convergence properties of the LAPW+LO basis and the different implementation of SOC effects, as discussed in section 1.3.2. However, the comparison of the PAW results in isolation demonstrates that the generation strategy of this work has significantly improved the convergence properties of the PAW basis sets of the early actinoids while maintaining the same quality.

2 Literatur

[1] M. Schlipf, F. Gygi, *Comput. Phys. Commun.* **2015**, *196*, 36–44.

[2] K. F. Garrity, J. W. Bennett, K. M. Rabe, D. Vanderbilt, *Comp. Mater. Sci.* **2014**, *81*, 446–452.

[3] A. Dal Corso, *Comp. Mater. Sci.* **2014**, *95*, 337–350.

[4] G. Prandini, A. Marrazzo, I. E. Castelli, N. Mounet, N. Marzari, *npj Comput. Mater.* **2018**, *4*, 1–13.

[5] P. Giannozzi et al, *J. Phys.: Condens. Matter* **2009**, *21*, 1–19.

[6] P. Giannozzi, O. Andreussi, T. Brumme, O. Bunau, M. Buongiorno Nardelli, M. Calandra *et al.*, *J. Phys.: Condens. Matter* **2017**, *29*, 465901.

[7] T. K. Sato, M. Asai, A. Borschevsky, T. Stora, N. Sato, Y. Kaneya *et al.*, *Nature* **2015**, *520*, 209–211.

[8] N. Troullier, J. L. Martins, *Phys. Rev. B* **1991**, *43*, 1993–2006.

[9] D. Vanderbilt, *Phys. Rev. B* **1990**, *41*, 7892–7895.

[10] K. Laasonen, A. Pasquarello, R. Car, C. Lee, D. Vanderbilt, *Phys. Rev. B* **1993**, *47*, 10142–10153.

[11] S. G. Louie, S. Froyen, M. L. Cohen, *Phys. Rev. B* **1982**, *26*, 1738–1742.

[12] D. J. Singh, L. Nordström, *Planewaves, Pseudopotentials, and the LAPW Method*, 2. Aufl., Springer, New York, NY, **2006**.

[13] L. Nordström, J. M. Wills, P. H. Andersson, P. Söderlind, O. Eriksson, *Phys. Rev. B* **2000**, *63*, 035103.

[14] J. Kuneš, P. Novák, R. Schmid, P. Blaha, K. Schwarz, *Phys. Rev. B* **2001**, *64*, 153102.

[15] A. Dal Corso, *Phys. Rev. B* **2010**, *82*, 075116.

[16] M. D. Jones, J. C. Boettger, R. C. Albers, D. J. Singh, *Phys. Rev. B* **2000**, *61*, 4644–4650.